Optical and EPR Spectral Investigation of VO(II) Doped in Aqualithiumaquabis(malonato)zincate Lattice

K Senthil Kumaran[1], S Boobalan[2,a] and G Sivasankari[3]*
[1,2]Research and Development Centre, Bharathiyar University, Coimbatore, India.
[1]Department of Chemistry, SNS College of Eng. Coimbatore, India.
[2,a] Department of Chemistry, VSB Engineering College, Karur, India.
[3]Department of Chemistry, Cauvery College for women, Trichy, India.

_____

ABSTRACT

Electron Paramagnetic Resonance studies are carried out at room temperature on single crystals of aqualithiumaquabis(malonato)zincate doped with VO(II) using X-band frequencies. Rotations in three mutually orthogonal planes indicate three chemically inequivalent sites, with intensities ratios of 1:2:9. However, only one site, with the highest intensity, could be followed during crystal rotations. The calculated spin Hamiltonian parameters are: gxx=1.976; gyy=1.973; gzz=1.933; Axx= 7.01 mT; Ayy= 6.77 mT; Azz= 18.01 mT. The impurity has entered the lattice in an interstitial position. The analysis of the powder spectrum also reveals the presence of only one site. Admixture coefficients, Fermi contact and dipolar interaction terms have also been evaluated. IR, UV-Visible and powder XRD data of doped complex confirm the structure and symmetry of the host lattice.

Keywords: Inorganic compound; Vanadyl; Crystal growth; Electron; Paramagnetic resonance; Location.

_____

INTRODUCTION

Electron Paramagnetic Resonance (EPR) studies in diamagnetic host lattices by incorporating paramagnetic transition metal ions provide information about the strength of the ligand field around the central metal atom. In these cases, the resonances are sharp due to the absence of dipole-dipole interaction. Vanadyl ion, i.e., VO(II), being one of the most stable molecular paramagnetic transition metal ion, it is widely used as an EPR probe to understand phase transitions, distortion, strength and magnitude of crystal fields, relaxation times, etc. Vanadium exists as bivalent, trivalent and tetravalent. Out of these, the ion commonly exists as VO(II), with a single unpaired 3d electron bound to an oxygen atom by strong bond in its tetravalent state. The orientation of the V=O bond in complexes depends on the nature of the ligands and hence shows very interesting results [1-4]. Most of the EPR results reported for this ion can be classified into two types, one in which the vanadyl ion freely rotates at normal temperatures and second category in which the ion is preferentially oriented. For example, if the ligands are water or sulfate ions, the vanadyl ion has fixed orientation, which in others, it has a random orientation. In addition, the analysis of the EPR spectra of VO(II) ion in various host lattices indicate that the paramagnetic impurity was found to enter the host lattice, predominantly as substitutionally [5-8]. However, interstitial position or both are also known [9,10]. The importance of malonato ligand in treating malignant tumors when coordinated with platinum is known (United States Patent 4140707). Coordination polymer compounds containing malonic acid as a ligand have been recently intensively studied due to their potential application as materials in molecular electronics, catalysts, biologically active compounds, molecular-based magnetic materials, microporosity, electrical conductivity, non-linear optical activity, etc. [11, 12]. Malonic acid acts as a ligand with various dentate abilities. Additionally, the

carboxylate group provides an efficient pathway that couples the magnetic centres either ferro- or antiferromagnetically [13-19]. In view of this importance of the ligand, the present single crystal EPR study of VO(II) in aqualithiumaquabis(malonato)zincate has been undertaken to identify the presence and nature of impurity in the host lattice.

EXPERIMENTAL SECTION

Material and Method
Preparation of single crystal of VO(II)-doped [Li(H2O)]2[Zn(mal)2(H2O)]
Malonic acid, zinc(II) basic carbonate, lithium hydroxide were purchased from commercial sources and used as received. [Li(H2O)]2[Zn(mal)2(H2O)] is synthesized by adding solid zinc(II) basic carbonate to an aqueous solution of malonic acid under continuous stirring. The suspension is heated at $40 - 50°$ C, until a colorless solution is obtained. This solution is filtered and mixed with an aqueous solution of lithium hydroxide. To this solution, five different concentrations of vanadyl sulfate (1.0, 1.5, 2.0, 2.5, and 5.0 %) are added as paramagnetic impurity. All the crystals are transparent and light blue color with well shaped and separated out on concentrating the solution at room temperature. Aqualithiumaquabis(malonato)zincate is abbreviated here as ALBZ.

EPR Measurements
EPR spectra are recorded at 300 K on a JEOL JES-TE100 ESR spectrometer operating at X-band frequencies, having a 100 kHz field modulation to obtain the first-derivative EPR spectrum. 1,1-Diphenyl-2-picrylhydrazyl (DPPH) with a g-value of 2.0036 is used as a reference for g-factor calculations.

UV-Visible, FT-IR, Powder XRD Measurements
The optical spectrum has been recorded at room temperature using a Varian Cary 5000 ultraviolet-visible (UV-Vis) near-infrared spectrophotometer in the range of 200-1300 nm. FT-IR spectra are recorded for doped and undoped materials on a Shimadzu FT-IR-8300/8700 spectrometer, in the frequency range of 4000-400 cm-1. The measurements are made using almost transparent KBr pellets containing fine-powdered samples at room temperature. Powder XRD studies are carried out for doped and undoped materials on a PANalytical X'pert PRO diffractometer with Cu Kα radiation of wavelength $\lambda = 0.15406$ nm, 2θ values between 5-75°, at room temperature.

Crystal structure
[Li(H2O)]2[Zn(mal)2(H2O)] is isostructural with [Li(H2O)]2[Cu(mal)2(H2O)] [20]. It belongs to triclinic crystal system with space group P1, having unit cell parameters a = 0.6851 nm, b = 0.8852 nm, c = 1.0529 nm, α = 80.65°, β = 75.04°, γ = 70.36° and Z = 2. The copper atom is five coordinated with a distorted square pyramidal environment. Four carboxylate-oxygen atoms from two crystallographically independent malonate groups build the equatorial plane around the copper atom. A water molecule occupies the apical position.

RESULTS AND DISCUSSION

Single crystal EPR studies
For a vanadyl impurity, along a crystallographic axis, an eight line pattern is observed since the electron spin is 1/2 and 51V nuclear spin is 7/2. In order to obtain spin Hamiltonian parameters at room temperature, single crystal rotations were performed along the three mutually orthogonal axes a*, b and c*, where axis b is the crystallographic axis b, axis a* is orthogonal to axis b in ab plane and axis c* is mutually perpendicular to both the axes b and a*. Crystals with 1 and 1.5% concentrations of dopant ion gave resonances that are relatively weak and hence difficult to follow during crystal rotations. However, in case of crystals with dopant ion concentration of 2.5 and 5.0%, the resonances are relatively broad. Hence, the former are used for XRD, whereas the latter are used for IR and UV-Vis studies. Hence, in the present EPR investigation, crystals with 2.0% are used for analysis. An EPR spectrum, when the applied magnetic field (B) is parallel to axis c* is shown in Fig. 1. Here, one can notice eight strong lines marked by the number (1-8), indicating that the ion under study is VO(II). However, additional resonance lines of

relatively lower intensity, are also seen, corresponding to other VO(II) sites in the lattice. As mentioned later, these lines could not be followed during crystal rotations, due to their lower intensity. Another EPR spectrum, recorded in a*c* plane, when B is 40° away from axis c* is given in Fig. 2. In this figure, the eight resonances corresponding to the higher intensity site which have been taken to calculate spin Hamiltonian parameters. Another EPR spectrum, when B is perpendicular to axis a* is shown in Fig. 3, which corresponds to the minimum spread. From the spectra obtained in the three orthogonal axes, isofrequency plots were plotted in the three orthogonal planes and are given in Figs. 4, 5 and 6 for a*c*, bc* and a*b planes respectively. These plots are on expected lines. In all these plots, the g minima and A minima are occurring at the same angle indicating that these two tensors are coincident..
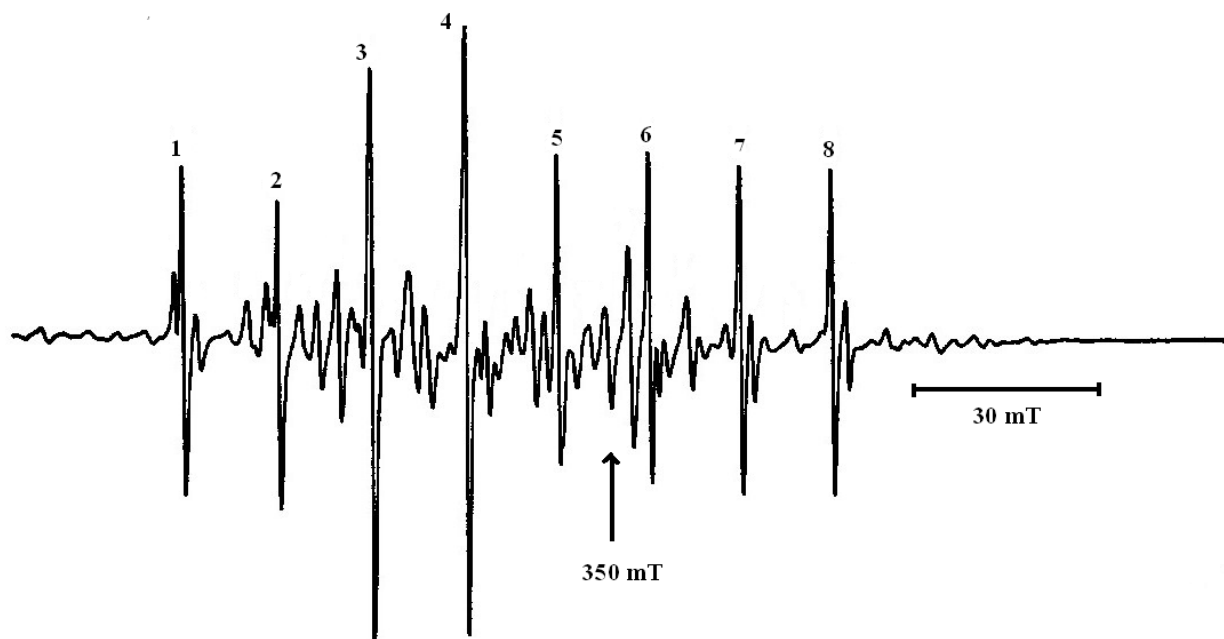

Figure 1: Single crystal EPR spectrum of VO(II)/ALBZ when the magnetic field (B) is parallel to axis c*. Frequency (v) = 9.08396 GHz. The strong lines marked by the numbers (1-8). Because of the low intensity we could not follow the small peaks

The spectra obtained in the three orthogonal planes for VO(II) ion were fitted with the following spin-Hamiltonian using the program EPR – NMR [21]

$$\hat{H}=\beta(g_xB_xS_x+g_yB_yS_y+g_zB_zS_z)+A_xS_xI_x+A_yS_yI_y+A_zS_zI_z \quad (1)$$

The g and A matrices thus calculated are given in Table 1, along with the principal values and direction cosines. It is clear from this Table that the direction cosines of the principal values of g and A are nearly coincident. The system shows rhombic symmetry, more so in g values. This point is also clear from isofrequency plot in a*b plane.
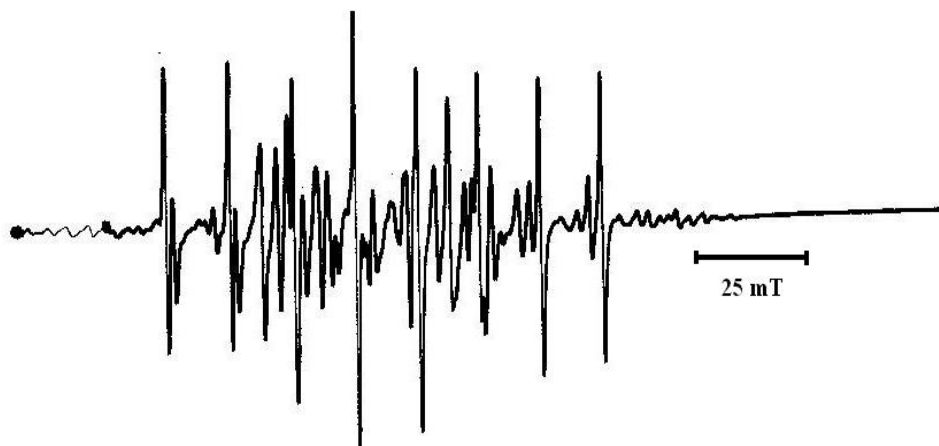
Figure 2: Single crystal EPR spectrum of VO(II)/ALBZ when the magnetic field (B) is 40° away from axis c* in a*c* plane. Frequency (ν) = 9.08606 GHz.
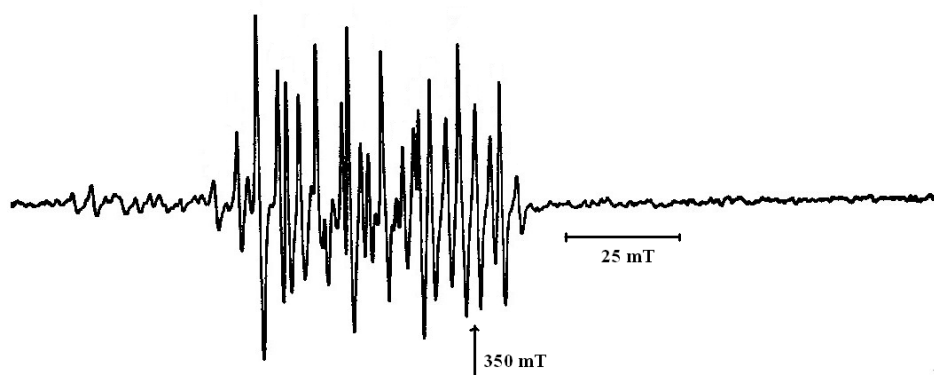

Figure 3: Single crystal EPR spectrum of VO(II)/ALBZ when the magnetic field (B) is perpendicular to orthogonal axis a* in a*b plane. Frequency (ν) = 9.08381 GHz.

In general, if a paramagnetic system exhibits axial symmetry, the isofrequency plots in a*c* and bc* planes will be indistinguishable, whereas the resonance lines in a*b plane show invariance. On the other hand, a slight deviation from axial symmetry makes the resonance lines in a*b plane show angular dependence. In the current system, the isofrquency plot in a*b plane is angle dependent and isofrequency plots in a*c* and bc* planes are not identical. This immediately confirms that the impurity has axial symmetry. Using these g and A matrices, the angular variation plots are simulated and are also given in Figs. 4, 5 and 6 respectively, where a good agreement is noticed. In all these figures, the solid lines indicate the theoretical values and the solid circles indicate the experimental values.

Table 1: Spin Hamiltonian parameters obtained from single crystal rotations for VO(II)/ALBZ using program EPR-NMR [21].

			Principal Values	Direction cosines		
				a*	b	c*
g matrix						
1.957	-0.001	-0.020	1.976	0.2036	-0.9679	-0.1473
	1.976	-0.000	1.973	-0.7461	-0.2508	-0.6168
		1.949	1.933	-0.6339	-0.0157	-0.7732
A matrix (mT)						
11.39	0.07	5.39	7.01	-0.2298	-0.9505	0.2093
	6.79	0.20	6.77	-0.7402	0.3103	0.5966
		13.61	18.01	0.6319	0.0178	0.7748
Powder spectrum						
$g_{\parallel} = 1.931$	$g_{\perp} = 1.985$		$A_{\parallel} = 19.94$ mT	$A_{\perp} = 7.84$ mT		

Table 2: Direction cosines of Zn-O bonds and Li-O bonds for ALBZ, obtained from crystallographic data [20]. [O(1), O(2), O(3) are belongs to one malonic acid O(11), O(12), O(13c) are belongs to another malonic acid. O(1w), O(2w) and O(3w) are belongs to water molecule.]

Zn-O, Li-O bonds in ALBZ	Direction cosines		
	a*	b	c*
Zn-O(1)	0.5639	0.4699	0.6791
Zn-O(11)	-0.2305	-0.5117	-0.8277
Zn-O(1w)	-0.8725	0.3130	0.3751
Zn-O(2)	0.0009	-0.8618	0.5072
Zn- O(12)	-0.2578	0.2959	-0.9198
Li(1)-O(2w)	0.6719	0.2344	0.7026
Li(1)-O(12)	-0.5568	-0.3946	-0.7309
Li(1)-O(1w)	-0.8715	-0.4609	0.1671
Li(1)-O(3)	-0.5056	0.4565	-0.7321
Li(2)-O(13c)	-0.3893	-0.1499	-0.9088
Li(2)-O(3w)	0.7796	0.5394	0.3183

The direction cosine of Zn – O bonds in ALBZ lattice are given in Table 2. These are helpful to predict the location of the paramagnetic impurity. If the direction cosines of principal value of g match with any one of the direction cosines of Zn – O bonds, one can assume that the dopant has entered the lattice substitutionally. Otherwise, an interstitial location is expected for the paramagnetic impurity. A close look at the direction cosines given in Tables 1 and 2 indicate that none of them matches with each other. In other words, one can suggest that the vanadyl ion might have entered the lattice in an interstitial location. In addition, the unit cell contains two molecules and in all the three planes, only one site is noticed during crystal rotations. This also suggests that the impurity has not entered substitutionally.
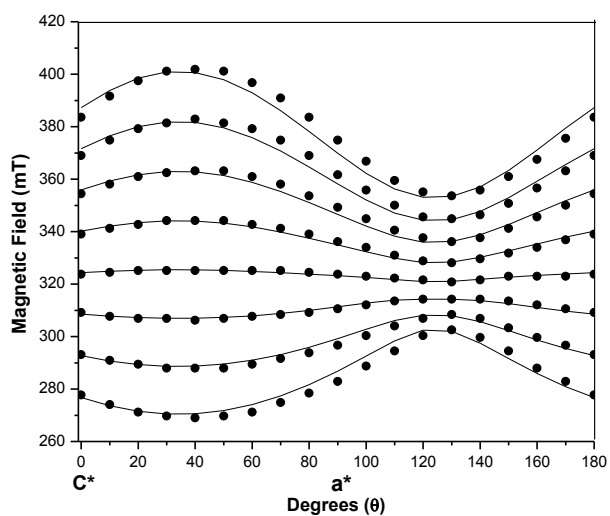
Figure 4 : Isofrequency plot of VO(II)/ALBZ in a*c* plane at room temperature. Solid circles indicate experimental values; solid lines correspond to theoretical values. Frequency (ν) = 9.08606 GHz
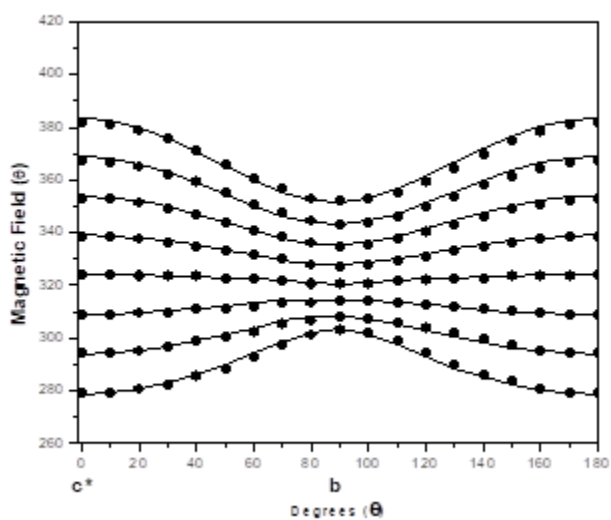
.

Figure 5: Isofrequency plot of VO(II)/ALBZ in bc* plane at room temperature. Frequency (ν) = 9.08396 GHz.
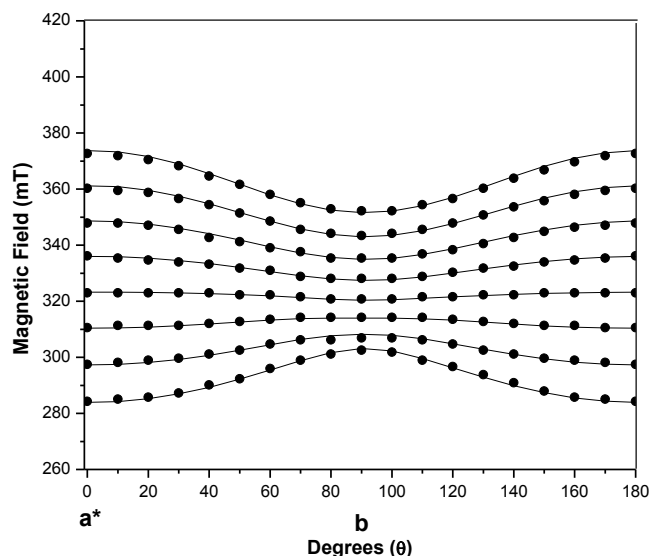
Figure 6: Isofrequency plot of VO(II)/ALBZ in a*b plane at room temperature. Frequency (ν) = 9.08381 GHz.

Polycrystalline EPR studies

The EPR spectrum of the powder sample of VO(II)/ALBZ, recorded at room temperature, is given in Fig. 7. The spin Hamiltonian parameters calculated from the powder spectrum are also given in Table 1.
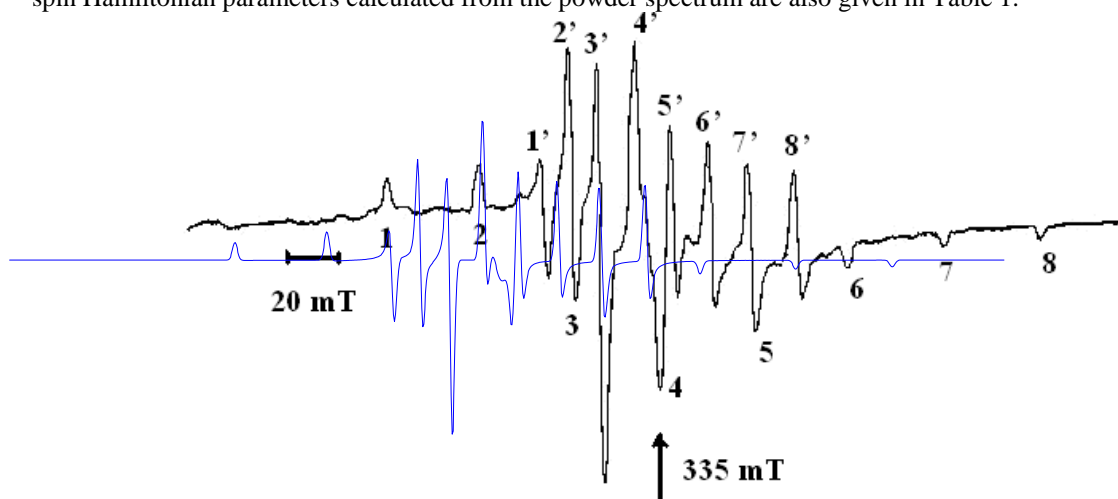

Fig. 7 Powder EPR spectrum of VO(II)/ALBZ at room temperature. The parallel components are marked by 1 to 8 and the perpendicular components are indicated by 1' to 8'. Top figure corresponds to experimental one, whereas bottom one is the simulated using parameters given in the text. Frequency (ν) = 9.38682 GHz.

The agreement between these values and the values obtained from single crystal analysis is relatively good. However, g_{xx}/g_{yy} and A_{xx}/A_{yy} are not resolved in powder spectrum due to the closeness in their values. This kind of observation is very common in VO(II) impurities. Using these parameters, the powder spectrum has been simulated and is also given in Fig. 7. The principal values of the spin-Hamiltonian parameters of VO(II) ion in ALBZ are tabulated with similar lattices in Table 3.

Table 3: Comparison of the principal values of spin-Hamiltonian parameters of the VO(II)/ALBZ with other lattices.

Lattice	Spectroscopic Splitting factor (g)			Hyperfine constant A (mT)			Ref.
	g_{zz}	g_{xx}	g_{yy}	A_{zz}	A_{xx}	A_{yy}	
PMZD[a]	1.936	1.978	1.972	18.24	7.12	6.73	[22]
DABMZ[b]	1.937	1.980	1.972	18.14	8.36	6.09	[23]
GeO$_2$	1.929	1.976	1.976	17.55	6.82	6.82	[24]
K$_2$TiO(C$_2$O$_4$)$_2$.2H$_2$O	1.940	1.972	1.972	16.30	6.00	6.00	[25]
ALBZ	1.933	1.976	1.973	18.01	7.01	6.77	Present Work

a - Dipotassium diaquabis(malonato-κ^2O,O') zincate dehydrate.

b - Diaquabis[malonato(1-) κ^2O,O'] zinc(II).

An octahedral complex exhibits $g\| < g\perp < g_e$ and $|A\|| > |A\perp|$, [26, 27] with a tetragonal compression. The value of $\Delta g\|/\Delta g\perp$ gives the tetragonality of VO(II) site where $\Delta g\|$ and $\Delta g\perp$ are deviation of $g\|$ and $g\perp$ from the free electron value, g_e (2.0023). In the present work, the value of $\Delta g\|/\Delta g\perp$ is greater than unity, indicating that the VO(II) ions are tetragonally distorted. The distortion takes place along V = O direction and the ground state of vanadium splits into dxy, dxz and dyz states.

Admixture coefficients:

The admixture coefficients are calculated from the spin-Hamiltonian parameters. The single unpaired electron on the metal ion occupies dxy or dxz or dyz orbital in an octahedral configuration. Upon lowering the symmetry, the ground state dxy can mix with dx2-y2, dyz and dxz. The admixture coefficients C1, C2 and C3 are related to the spin-Hamiltonian parameters by the relations [28]

$$g\| = 2\left(3C_1^2 - C_2^2 - 2C_3^2\right); \quad (2)$$

$$g_\perp = 4C_1\left(C_2 - C_3\right) \quad (3)$$

The equations (2) and (3) along with the normalization condition $\left(C_1^2 + C_2^2 + C_3^2 = 1\right)$ can be solved iteratively to obtain the admixture coefficients. The values that obtained are given in Table 4, along with few literature values.

Table 4: Orbital admixture coefficients and bonding parameters of vanadyl ion in various systems.

Host lattice	C_1	C_2	C_3	κ	$P \times 10^{-4}$ cm^{-1}	Ref.
MPSH[c]	0.7000	0.7130	0.0704	0.85	133.1	[29]
MPPH[d]	0.7014	0.7128	0.0067	0.83	130.7	[30]
MAPH[e]	0.7019	0.7111	0.0400	0.91	112.0	[1]
CPPH[f]	0.7015	0.7115	0.0016	0.77	141.9	[2]
ZSPH[g]	0.7012	0.7118	0.0016	0.84	133.8	[31]
ALBZ	0.7012	0.7118	0.0403	0.81	130	Present Work

c - Magnesium Potassium Sulphate Hexahydrate.

d - Magnesium Potassium Phosphate Hexahydrate.

e - Magnesium Ammonium Phosphate Hexahydrate.

f - Cadmium Ammonium Phosphate Hexahydrate.

g - Zinc Sodium Phosphate Hexahydrate.

Optical absorption studies:

The optical absorption spectrum of VO(II) doped in ALBZ at room temperature is shown in Fig. 8. The spectrum consists of three absorption bands at 327 nm (30,581 cm-1), 575 nm (17,391 cm-1) and 700 nm (14,285 cm-1) respectively. VO(II) ion with d1 configuration has 2D ground state.
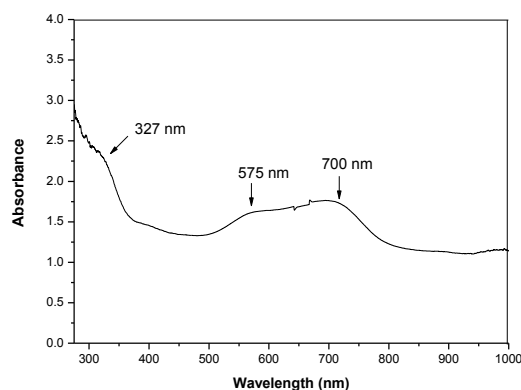
Figure 8: Optical absorption spectrum of VO(II)/ALBZ at room temperature

In octahedral crystal field, the 2D state splits into 2T2g and 2Eg, while an octahedral field with tetragonal distortion further splits the 2T2g level into 2Eg and 2B2g, and 2Eg level splits into 2A1g and 2B1g. Among these levels, B2g will be the ground state. Thus, for VO(II), two bands are expected corresponding to the transitions 2B2g → E2g and

2B2g → 2B1g. These two bands can be assigned to $\Delta^\perp$ = 2B2g → E2g (Edxy→dxz, dyz) and $\Delta\|$ = 2B2g → 2B1g

(Edxy→dx2-y2) transitions respectively. Except for the high – energy band at 30,581 cm-1, all other bands are attributed as d-d transitions. The band at 30,581 cm-1 is due to charge transfer, arising from the promotion of electron from the filled bonding level (oxygen orbital) eπb to nonbonding level b2 and is assigned to the transition eπb→ 2B2g (b2) (from filled level to dxy level) [32].

Both EPR and optical data can be used to calculate the molecular orbital coefficients by using following equations [33, 34],

$$g\| = g_e \left[1 - \frac{4\lambda \beta_1^2 \beta_2^2}{\Delta\|}\right] \qquad (4)$$

$$g_\perp = g_e \left[1 - \frac{\lambda \gamma^2 \beta_2^2}{\Delta_\perp}\right] \qquad (5)$$

Here ge is free electron g value equal to 2.0023 and λ is the free ion value of the spin-orbit coupling constant of

VO(II) ion (170 cm-1 [35]). β_1^2, β_2^2 and γ2 are the molecular orbital coefficients of the d1 electron. These molecular orbital coefficients (also called bonding coefficients) thus characterize in-plane σ bonding, in-plane π bonding and out-of-plane π bonding, respectively.

The parallel and perpendicular components of hyperfine interaction A$\|$ and A$^\perp$ are related to the molecular orbital coefficients by the following expressions [36],

$$A\| = -P[\kappa - 4/7 \, \beta_2^2 - (g_e - g\|) - 3/7(g_e - g\perp)] \qquad (6)$$

$$A\perp = -P[\kappa - 2/7 \, \beta_2^2 - 11/14(g_e - g\perp)] \qquad (7)$$

The degrees of distortion can be estimated from the Fermi contact term κ and the P parameter, which are related to

radial distribution of wave function of the ions given as   P = gegNβeβN(r-3). Here, β_2^2 is the covalency ratio of V=O bonds. The parameter P is related to the isotropic hyperfine coupling and represents the amount of unpaired electron density at the nucleus.

Neglecting the second order effects and taking negative values for A$\|$ and A$^\perp$, P value is calculated from Eq. (8) [37] and the results are given in Table 4.

$$P = 7(A\| - A\perp)/6 + (3/2)(\lambda/\Delta\|) \qquad (8)$$

The Fermi contact parameter (κ) is calculated by using the equation

$$\kappa = -A_{iso}/P - (g_e - g_{iso}) \qquad (9)$$

Here, A_{iso} and g_{iso} are calculated from the powder A and g values respectively.   Combining Eqs. (6) and (7) and eliminating κ, one can get an expression for β_2^2 in terms of the principal values of the g and A tensors,

$$\beta_2^2 = (-7/6)[(A\| - A\perp)/P + (g_e - g\|) - (5/14)(g_e - g\perp)] \quad (10)$$

The calculated parameters are given in Table 5. The deviation of β_1^2 from unity usually represents the degree of the admixture of the ligand orbitals and increase in the degree of covalency. β_1^2, found in this work, clearly indicates that the bonding is nearly ionic and represents poor π bonding of the ligands. If β_1^2 = 1, the bond would be completely ionic. If β_1^2 = 0.5, the bond would be completely covalent. The parameters 1 - β_1^2 and 1 - γ2 are the measures of the covalency. First term gives an indication of the influence of σ bonding between vanadium atom and equatorial ligands, second indicates the influence of π bonding between the vanadium ion and the vanadyl oxygen.

Table 5: Molecular orbital coefficients for VO(II) ion in the lattices .

Systems	β_1^2	β_2^2	γ^2	Ref.
		LAM		
Site I	0.26	1	0.62	[10]
Site II	0.68	1	0.95	
PMZD	0.78	-	0.74	[22]
DABMZ	0.76	-	0.58	[23]
MPPH	0.84	-	0.89	[30]
ALBZ	0.86	0.84	0.91	Present work

FT-IR spectral studies

 Fourier transform infrared spectroscopy is employed to identify the nature of the bonding between various groups, a shift in the stretching and bending vibrations is generally observed. The FTIR spectra of pure and VO(II) doped ALBZ at room temperature are shown in Fig. 9. Experimental FTIR bands and their faltering assignments [38] for unpolluted ALBZ and VO(II) doped ALBZ are tabulated in Table 6.
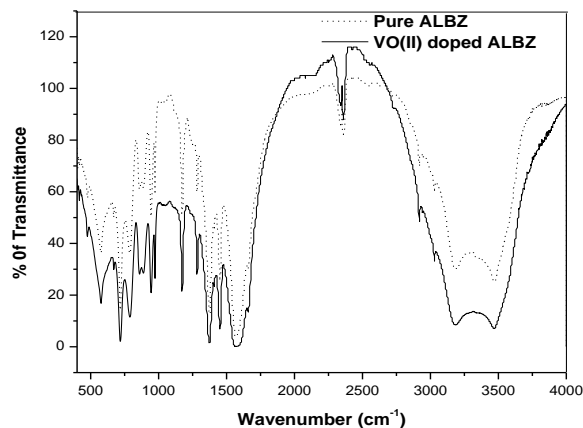

Figure 9: FT-IR Spectrum of VO(II)/ALBZ at room temperature.

Table 6: Observed FT-IR bands and their tentative assignments for Pure ALBZ and VO(II)/ALBZ.

Assignments	FT-IR bands (cm^{-1})	
	Pure ALBZ	VO(II) doped ALBZ
Zn – O	401	419
Zn – O + O – C = O	789	787
- OH	3468, 3182	3470
....OH$_2$	3029	3029
Zn – OH$_2$	718, 789	665, 723
	885, 945	947
-CH$_2$-	2921	2923
-C = O	1175, 1285	1180, 1256
	1570, 2152	1728

Powder XRD studies

      Powder XRD of VO(II) doped ALBZ at room temperature is shown in Fig. 10. The powder XRD is used to identify and characterize the powder sample, in the crystalline materials. Based on powder XRD results, the VO(II) doped ALBZ powder sample has identical lattice parameters as the pure ALBZ powder sample. The lattice parameters are tabulated in Table 7 with the single crystal XRD parameter of ALBC [20]. It is apparent from the table that the parameters of pure ALBZ and VO(II) doped ALBZ corresponding with reported values of copper complex [20], signifying that the zinc and copper complexes are isomorphic and the low impurity concentration does not alter the structure and symmetry of the host lattice.
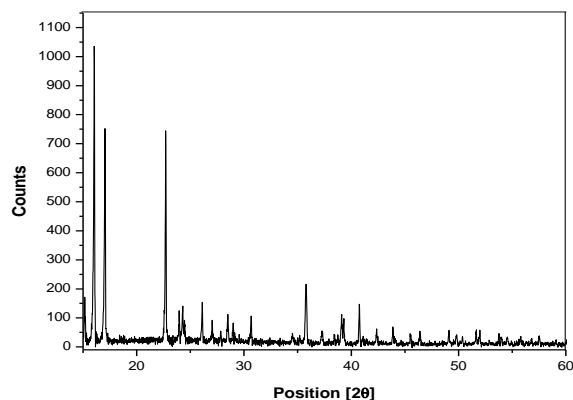

Figure 10: Powder XRD pattern of VO(II)/ALBZ at room temperature.

Table 7: Calculated lattice parameters of ALBZ and VO(II)/ALBZ from powder XRD, along with single crystal XRD of ALBC [20].

Lattice parameters (nm) of ALBC from single crystal XRD	Lattice parameters (nm) calculated from powder XRD	
	ALBZ	VO(II) doped ALBZ
a = 0.6851	a = 0.6382	a = 0.6382
b = 0.8852	b = 0.8424	b = 0.8424
c = 1.0529	c = 1.0293	c = 1.0293

CONCLUSION

Single crystal EPR technique is used to study the vonadyl ion doped ALBZ. The results indicate more than one site in the lattice and the number of sites seems to be independent of concentration of the impurity. Spin Hamiltonian parameters point out that the impurity is axially indistinct and entered the lattice in an interstitial position. The isofrequency plots and the powder EPR spectrum have been simulated, which authenticates evaluated spin Hamiltonian parameters. The optical absorption spectrum at room temperature shows three bands characteristic of vanadyl ions in distorted octahedral symmetry. Admixture coefficients, molecular orbital coefficients, Fermi contact term and dipolar interaction parameter have also been calculated. FTIR and XRD studies confirm the formation and structure of the complex.

REFERENCES

[1]   I.Sougandi; R.Venkatesan; T.M.Rajendran; Sambasiva Rao P. *Phy Scripta .* **2003**, 67, 53-58.
[2]   I.Sougandi; T.M. Rajendran; R.Venkatesan; Sambasiva Rao P. *Proc Indian Acad Sci. (Chem. Sci.).* **2002**, 114, 473-79.
[3]   I.Sougandi; R.Venkatesan; P.Sambasiva Rao. *J Phys Chem Solids.* **2003**, 64, 1231-36.
[4]   R.Tapramaz; B.Karabulut; F.Koksal. *J Phys Chem Solids*. 2000, 61, 1367-74.
[5]   A. Kasiviswanath; S.Radhakrishna. *J Phys Chem Solids.* **1991**, 52, 232-40.
[6]   S.K.Misra; C.Wang. *Physica B*. **1989**, 159, 321-28.
[7]   B.Venkatraman. *Ind J Pure & Appl Phys*. **1996**, 34, 273-80.
[8]   M. Venkateshwarlu; T. Bhaskar Rao; A.Hussain. *Phys Stat Sol*, **1994**, 31,185-93.
[9]   B. Deva Prasad Raju; K.V.Narasimhulu; N.O.Gopal, Lakshmana Rao J. *J Phys Chem Solids*. **2003**, 64, 1339-45.
[10]   Ram Kripal; Indrajeet Mishra; Gupta S.K; Manju Arora. *Spectrochim. Acta A*. **2009**, 71, 1969-76.
[11]   C.Ruiz-Perez; Rodriguez-Martin Y; Hernandez-Molina M; Delgado F.S; Pasan J; Sanchiz J;Lloret F; Julve M. *Polyhedron*. **2003**, 22, 2111-19.
[12]   J.Pasan; F.S.Delgado; Y.Rodriguez-Martin; M. Hernandez-Molina; C.Ruiz-Perez; J.Sanchiz; F.Lloret; Julve M. *Polyhedron*. **2003**, 22, 2143-51.
[13]   C. Oldham, G. Wilkinson, R.D. Gillard, J.A. McCleverty (Eds.). Comprehensive Coordination Chemistry. Pergamon Press, Oxford, **1987**, 2, 435-42.
[14]   D.K. Towle; S.K. Hoffmann; W.E. Hatfield; P. Singh; P.Chaudhuri. *Inorg Chem*. **1988**, 27, 394-401.
[15]   P.R. Levstein; R. Calvo. *Inorg Chem*. **1990**, 29, 1581-89.
[16]   F. Sapina; E. Escriva; J.V. Folgado; A. Beltra´n; A. Fuertes; M. Drillo. *Inorg Chem*. **1992**, 31,3851-59.
[17]   E. Colacio; J.P. Costes; R. Kiveka¨s; J.P. Laurent; J. Ruiz. *Inorg Chem,* **1990**, 29, 4240-48.
[18]   E. Colacio, J.M. Domı´nguez-Vera, J.P. Costes, R. Kiveka¨ s,J.P. Laurent, J. Ruiz, M. Sundberg, Inorg. Chem. 1992, (31) 774-80.
[19]   E. Ruiz. *Inorg Chem*. **1993**, 212, 115-22.
[20]   F.S.Delgado Ruiz; C. Sanchiz J; Lloret F; Julve M. *Cryst Eng Comm*. **2006**, 8, 507-16.
[21]   F. Clark; Dickson R.S; Fulton O.B; Isoya J; Lent A; Mc Gavin D.G; Mombourquette M.J; Nuttall R.H.D; Rao P.S; Rinnerberg H; Tennant W.C; Weil J.A. EPR-NMR Program, University of Saskatchewan, Saskatoon, Canada, **1996**.
[22]   B.Natarajan; Mithira S; Deepa S; Ravikumar R.V.S.S.N; Sambasiva Rao P. *Rad Eff Def Solids*. 2006, 61, 177-83.
[23]   B.Natarajan; Mithira S; Deepa S; Ravikumar R.V.S.S.N; Sambasiva Rao P. *J Phys Chem Solids,* **2007**, 68, 1995.
[24]   I. Siegel. *Phys Rev*. **1964**, 193, 134-41.
[25]   R.M. Golding. *Mol Phys*. **1962**, 5, 369-76.
[26]   A. Abragam, Bleaney B. Electron Paramagnetic Resonance of Transition Ions, Clarendon, Oxford, **1970**.
[27]   A.Murli; Rao J.L; Subbaiah A.V. *J Alloys Compd*.**1997**, 257, 96-102.
[28]   V.P.Seth; Yadav S.K; Jain V.K; Pramana, *J Phys*.**1983**,21,65-71.
[29]   H. Anandalakshmi; T.M. Rajendiran; R.Venkatesan; P Sambasiva Rao. *Spectrochimi. Acta*. **2000**, 56, 2617-22.
[30]   R. Poonguzhali; R.Venkatesan; T.M. Rajendiran; P. Sambasiva Rao ; Ravikumar R.V.S.S.N; Reddy Y.P., Cryst. Res. Technol. 2000, (35) 1203-08.
[31]   K.Velavan, I. Sougandi R.Venkatesan, P.Sambasiva Rao, J. Phys. Chem. Solids 2005, (66) 15-21.

[32]   A.B.P. Lever., Inorganic electronic spectroscopy, 2nd ed; Elsevier: New York, 1986 Chapter 4.

[33] V.P. Seth, S.Gupta, A. Jindal, S.K.Gupta, J. Non-Cryst. Solids 1993, (162) 263.

[34] R.Muncaster, S. Parke, J. Non-Cryst. 1977, (24) 399-404.

[35] C.J. Ballhausen, B H.B.Gray, Inorg. Chem. 1961, (1) 111.

[36] D.Pathinettam Padiyan, C.Muthukrishnan, R., J. Murugesan Mol. Struct. 2003 (648) 1-9.

[37] U.B.Gangadharmath, S.M.Annigeri, A.D. Naik, V.K. Revankar Mahale J. Mol. Struct. (Theochem.) 2000, (572) 61-69.

[38] K.Nakamoto, P.J. McCarthy Ruby, A., Martell A.E., J. Am. Chem. Soc., 1961, (83) 1066-72.